Biomaterials 35 (2014) 9236–9245

Contents lists available at ScienceDirect

Biomaterials

journal homepage: www.elsevier.com/locate/biomaterials

Collagen mimetic peptide engineered M13 bacteriophage for collagen targeting and imaging in cancer

Hyo-Eon Jin [a, b], Rebecca Farr [a, b], Seung-Wuk Lee [a, b, *]

[a] Department of Bioengineering, University of California, Berkeley, CA 94720, USA
[b] Physical Bioscience Division, Lawrence Berkeley National Laboratory, Berkeley, CA 94720, USA

ARTICLE INFO

Article history:
Received 1 June 2014
Accepted 23 July 2014
Available online 10 August 2014

Keywords:
Collagen
Bacteriophage
Cancer
Targeting
Imaging

ABSTRACT

Collagens are over-expressed in various human cancers and subsequently degraded and denatured by proteolytic enzymes, thus making them a target for diagnostics and therapeutics. Genetically engineered bacteriophage (phage) is a promising candidate for the development of imaging or therapeutic materials for cancer collagen targeting due to its promising structural features. We genetically engineered M13 phages with two functional peptides, collagen mimetic peptide and streptavidin binding peptide, on their minor and major coat proteins, respectively. The resulting engineered phage functions as a therapeutic or imaging material to target degraded and denatured collagens in cancerous tissues. We demonstrated that the engineered phages are able to target and label abnormal collagens expressed on A549 human lung adenocarcinoma cells after the conjugation with streptavidin-linked fluorescent agents. Our engineered collagen binding phage could be a useful platform for abnormal collagen imaging and drug delivery in various collagen-related diseases.

Published by Elsevier Ltd.

1. Introduction

Collagen is one of the most important extracellular matrix (ECM) proteins that plays a critical role in various biological functions including cell attachment, differentiation, and migration, as well as maintenance of tissue mechanical integrity [1,2]. Abnormal collagen remodeling occurs in various diseases such as cancer, tissue fibrosis, Marfan syndrome, etc. [3–5]. Recently, abnormal collagen remodeling has attracted a lot of attention in cancer diagnostics and therapeutics because an increase in abnormal collagen remodeling is correlated with the long-term survival rate of human cancer patients [5–8]. Moreover, many types of collagen are over-expressed in different cancers: collagen type I in breast cancer and medulloblastoma [7–9], collagen type I and III in ovarian cancer [10], collagen type IV in pancreatic cancer [11], and collagen type IV and VII in colorectal cancer [12]. Therefore, collagen is emerging as a biomarker for cancer diagnosis and as a predictor of cancer prognosis [11].

Collagen is composed of three polypeptide chains, containing the repeating amino acid motif (Gly-X-Y), where X and Y can be any amino acid, to form a triple-helical structure [13]. A single collagen fiber is 300 nm in length and 1.5 nm in width. They form collagen fibrils that exhibit a characteristic repeating banding pattern with a periodicity of 64–67 nm, depending on the tissue [13,14]. Interstitial collagens are resistant to most proteolytic enzymes, but vertebrate collagenases (i.e., matrix metalloproteinases, MMPs) cleave them at a single site, approximately three-quarters of the length from the N-terminus of the triple helix [15–17]. The expression and activity of MMPs are increased in almost every type of human cancer, and this correlates with advanced tumor stage, increased invasion and metastasis, and shortened survival rates [16–18]. The over-expression of collagen paired with the over-expression of MMPs during cancer progression causes abnormal collagen remodeling to occur. Therefore, collagen in cancers has highly degraded, branched, and denatured structures, which differ from normal collagen structures [19]. These abnormal disrupted collagen structures can be unique targets for cancer imaging or therapeutics [5,20].

Genetic engineering of bacteriophages (phages) provides unprecedented opportunities for building nanomaterials for biomedical applications, including drug/gene delivery and tissue engineering [21–29]. Specifically, M13 phage has a filamentous shape (880 nm in length and 6.6 nm in diameter for wild type), composed of single stranded DNA that is encapsulated by 2700 copies of the major coat protein pVIII and capped on both ends with

* Corresponding author. Department of Bioengineering, University of California, Berkeley, CA 94720, USA. Tel.: +1 510 486 4628; fax: +1 510 486 6488.
E-mail address: leesw@berkeley.edu (S.-W. Lee).

http://dx.doi.org/10.1016/j.biomaterials.2014.07.044
0142-9612/Published by Elsevier Ltd.

5 copies of four different minor coat proteins, pIII, pVI, pVII, and pIX (Fig. 1A). These subunit proteins can be engineered to display various functional peptides, such as RGD (integrin-binding peptide), IKVAV (neural cell stimulating peptides), DGEA (bone-cell stimulating peptides), and PmpD (Polymorphic Membrane Protein D from *Chlamydia trachomatis*), on the major and minor coat proteins of the phage through genetic modification [22,26,27,30,31]. The phages have an advantageous nanoscale size and the capability for multivalent and orthogonal display. A phage can deliver a large payload ($>1.5 \times 10^{13}$ epitopes/cm^2) of therapeutic molecules without compromising its integrity [26,32–35].

In this paper, we developed an engineered M13 phage with two functional peptides (collagen and streptavidin binding peptides) and characterized the efficiency of the engineered phage in targeting and imaging cancer-related collagens (Fig. 1). Collagen mimetic peptide (CMP) and streptavidin binding peptide (HPQ) were chosen to be expressed on the pIII minor coat protein and pVIII major coat protein of M13 phage, respectively. CMP peptide (Gly-Pro-Pro repeats; 7GPP) is the most conserved amino acid sequence of natural collagen and exhibits strong affinity to collagen [36,37]. Streptavidin binding peptide motif (His-Pro-Gln, HPQ) allows binding to streptavidin-conjugated molecules for imaging or for use as therapeutic agents. We compared the binding affinity of CMP engineered phages to various collagens including normal type I collagen as well as disrupted, heat-denatured, and MMP1-treated type I collagen. We hypothesized that the fluorescent-conjugated CMP engineered phage could be used to target and image abnormal collagen in A549, human lung adenocarcinoma cells.

2. Materials and methods

2.1. Genetic engineering of M13 phages

M13 phage major and minor coat proteins were engineered using an inverse polymerase chain reaction (PCR) cloning method as previously reported [29,38]. For the M13-nGPP construct (*n*: number of inserts), the gIII reverse primer was designed to include the EagI restriction site, the insert sequence, and a segment complimentary to the gIII 5′–3′ strand. The gIII forward primer was designed to make the vector linear and was fully complimentary to the engineered gIII 3′–5′ region, including an EagI restriction site (Supplementary Table S2, for primer sequences). To incorporate the gene sequences, PCR was performed using Phusion™ High-Fidelity DNA Polymerase, the two primers, and an M13KE phage vector (New England Biolabs, Ipswich, MA). The obtained product was purified on an agarose gel, eluted with spin column purification, digested with EagI enzyme (New England Biolabs), and ligated overnight at 16 °C with T4 DNA Ligase (New England Biolabs). For the M13-7GPP$_{III}$, g3-7GPP and g3-Ext primers were annealed together to make 7GPP insert. The resulting gene was then restricted by KpnI (New England Biolabs) and EagI enzyme. The 7GPP insert and restricted M13KE vector were ligated overnight with T4 DNA Ligase. The ligated DNA vector was then electroporated into XL1-Blue® electrocompetent cells (Stratagene, La Jolla, CA), and the amplified plasmid was verified by DNA sequencing at the University of California Berkeley DNA Sequencing Facility (Berkeley, CA) (Supplementary Table S1, for phage sequences). M13-HPQ$_{VIII}$ construction methods were used as described previously (Supplementary Table S2, for primer sequences) [23].

2.2. Phage amplification and purification

To amplify engineered M13 phages, a culture of XL1-Blue (Stratagene, La Jolla, CA) was grown overnight in tetracycline antibiotic. The following day, a freshly picked plaque of M13 phages was grown in a 1:100 dilution of XL1-Blue in selective media to midlog phase. Cultures were centrifuged at 10,000 rpm for 20 min. Supernatants were collected, and phage were precipitated overnight at 4 °C with 20% PEG8000/2.5 M NaCl. After centrifugation, phage was resuspended in a final 1 mL of 50 mM TBS and tittered by UV–Vis spectrometry or plaque forming assay.

2.3. Collagen assembly

To prepare the differently structured collagen samples for the binding experiments, a collagen solution (3 mg/mL, type I rat tail, Gibco) was diluted to 2 mg/mL in 0.1 M citrate buffer, pH3 or pH6, for the highly branched and normal collagen nanostructures, respectively. Collagen coated films on gold substrate were constructed at pulling speed 10 μm/min using biomimetic nanofiber assembly process that we developed previously [25]. Atomic force microscopy (AFM) images were obtained in a tapping mode in air using an AFM (MFP3D, Asylum research, Santa Barbara, CA).

2.4. Phage binding assays on collagen films

Collagen solution (3 mg/mL, type 1 rat tail, Gibco) was diluted with 0.1 M citrate buffer, pH3 or pH6, and 10 μg of collagen (50 μl) was added to a 96-well plate (Costar) and air-dried to make collagen film. For MMP1 treated collagen film, collagen solution (pH3) was added to the plate and air-dried, and then Recombinant Human MMP-1 Catalytic Domain (BioVision, Milpitas, CA) in buffer (ENZO Life

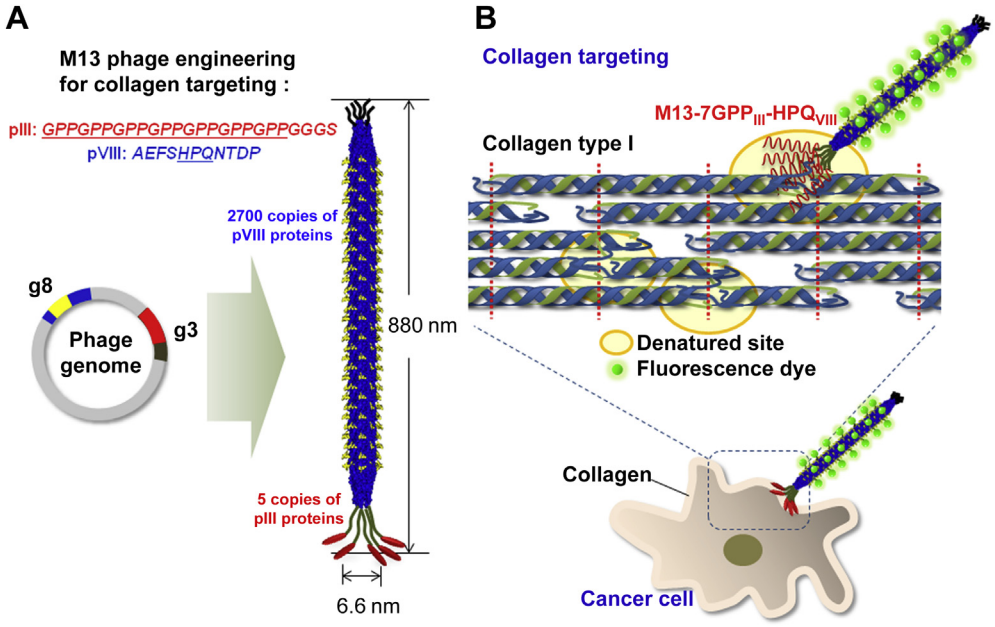

Fig. 1. Schematic of the collagen-mimetic peptide engineered M13 phage construction and its application for abnormal collagen imaging. (A) The phage expresses 2700 copies of HPQ (biotin-like peptide) motif on its pVIII major coat proteins and 5 copies of 7GPP (hepta-repeats of Gly-Pro-Pro) motif on its pIII minor coat proteins (termed M13-7GPP$_{III}$-HPQ$_{VIII}$). (B) The collagen mimetic peptide engineered phage will target the disrupted collagen. The fluorescent dyes (green circles) labeled CMP engineered phage will target and image collagens in cancer cells. The schematic illustration of the collagens and phages are not to scale. (For interpretation of the references to color in this figure legend, the reader is referred to the web version of this article.)

Sciences, Farmingdale, NY) was treated on collagen films in the plate for 2 days at room temperature. To make gelatin films, the same collagen solution was denatured at 70 °C for 15 min, and 10 μg of collagen (50 μl) was added to a 96-well plate and air-dried. The 96-well plates were blocked with 1% BSA in PBS for 1 h and washed three times with PBS. Phages (1.0×10^{10} phages/mL) were incubated in collagen film for 1 h at 37 °C and washed three times with PBS. We measured binding phages by ELISA assay as previously described with modifications [23]. 200 μl of diluted HRP-conjugated anti-M13 monoclonal antibody (GE Healthcare, Piscataway, NJ) (1:5000 dilution in blocking buffer) was treated to each well and incubated at room temperature for 1 h with agitation. Plates were washed with PBST five times, then incubated with 3,3′,5,5′-Tetramethylbenzidine (TMB) liquid substrate (Sigma Aldrich, St. Louis, MO) at room temperature for 10–30 min and treated with the same amount of stop reagent (Sigma Aldrich, St. Louis, MO). The absorbance was measured using a microplate reader (Safire, Tecan Group Ltd., Männedorf, Switzerland) set at 450 nm.

2.5. Phage binding assays on various collagen types

We performed binding assay for various collagen types. Rat collagen type I (Gibco, Island, NY), human collagen type I (Sigma Aldrich, St. Louis, MO), bovine collagen type II (Sigma Aldrich, St. Louis, MO), human collagen type III (Sigma Aldrich, St. Louis, MO), human collagen type IV (Sigma Aldrich, St. Louis, MO), and human collagen type V (Sigma Aldrich, St. Louis, MO) were diluted with 100 mM citrate buffer pH3, and 10 μg of collagen (50 μl) was added to a 96-well plate (Costar) and air-dried. Phages (1.0×10^{10} phages/ml) were incubated in collagens for 1 h at 37 °C. ELISA method was same as described above in 2.4. Phage binding assays on collagen films.

2.6. A549 human lung cancer cell culture

A549, human lung adenocarcinoma cells, were cultured in T-75 flask (Nunc, Rochester, MN) in DMEM containing 10% FBS, 2 mM L-glutamine, 100 U/ml penicillin and 100 μg/ml streptomycin at 37 °C in a humidified 5% CO_2 atmosphere, and the growth media was changed every 2 days. 5×10^3 cells were seeded in a 96 well plates for ELISA study, and 1×10^4 cells were seeded in a Lab-Tek®II CC2 Chamber Slide™ (Thermo-Fisher Scientific, Rochester, NY) for collagen imaging. For collagen induction, the cells were incubated in the presence of 5 ng/ml of TGF-β1 and 5 μg/ml of L-ascorbic acid for 72 h [39].

2.7. RT-PCR to measure collagen expression

Total RNA was isolated using Trizol (Invitrogen, Carlsbad, CA) and RT-PCR was performed using the SuperScript One-Step RT-PCR kit (Invitrogen). The target transcript was reverse transcribed at 50 °C for 30 min. For type I collagen, the PCR product was amplified using 30 cycles (initial denaturation at 94 °C/2 min followed by PCR amplification, 94 °C/30 s, 58 °C/30 s, and 68 °C/1 min) [39]. PCR products were visualized on a GelDoc system (Bio-Rad, Hercules, CA) and band density was analyzed using NIH ImageJ. The following primers were used for PCR: human collagen type I forward (5′-ACGTCCTGGTGAAGTTGGTC-3′), human collagen type I reverse (5′-ACCAGGGAAGCCTCTCTCTC-3′), human GAPDH forward (5′-GGGCTGCTTTTAACTCTGGT-3′), and human GAPDH reverse (5′-TGGCAGGTTTTTC-TAGACGG-3′).

2.8. Gelatin zymography for matrix metalloproteinases (MMPs) expression in A549 cells

We measured the expression level of MMPs by TGF-β1 and L-ascorbic acid treatment in the cell culture media using gelatin-based zymography. Cells (1.5×10^4 cells/well) were seeded in a 48-well plate and stimulated with 5 ng/ml of TGF-β1 and 5 μg/ml of L-ascorbic acid for 72 h, and media were collected. After measuring the protein concentration by BCA assay, equal amounts (50 μg) of samples were mixed with an equal volume of 2× non-reducing sample buffer (Bio-Rad, Hercules, CA). The samples were applied to a 10% Ready Gel® Zymogram Gel (Bio-Rad, Hercules, CA). After electrophoresis, SDS was removed from the gel by washing 3 times for 10 min in 2.5% Triton X-100 solution. Then the gels were incubated overnight with gentle shaking at 37 °C in buffer [50 mM Tris–HCl (pH 7.6), 10 mM $CaCl_2$, 50 mM NaCl, 0.05% Brij35], and then the gel was stained with 0.25% Coomassie blue R250 in 40% methanol and 10% acetic acid for 2 h at room temperature and subsequently destained with a 40% methanol, 10% acetic acid solution until the bands became clear.

2.9. Conjugation of streptavidin-Alexa Fluor®488 on the phage for imaging

M13-HPQ_{VIII} and M13-$7GPP_{III}$-HPQ_{VIII} phages (10^{14} phages each) were mixed with 100 μL of 2 mg/mL Streptavidin-Alexa Fluor®488 and incubated for 1 h at room temperature under gentle mixing. The phages were PEG-precipitated twice and resuspended in 400 μL of PBS. After conjugation, the amount of Streptavidin-Alexa Fluor®488 per phage was measured by UV–Vis at 269 nm and 495 nm. Streptavidin-Alexa Fluor®488 conjugated phages were used for fluorescence microscopy and fluorescence-activated cell sorting (FACS) analysis.

2.10. Fluorescence microscopy for collagen imaging in A549

Chamber slides were blocked with 1% BSA in the cell culture media for 1 h before phage treatment, and then 1.0×10^{10} phages/mL were incubated with cells for 1 h at 37 °C. Alexa Fluor® 488 conjugated M13-$7GPP_{III}$-HPQ_{VIII} phages and Alexa Fluor® 488 conjugated M13-HPQ_{VIII} (control) were treated onto the TGF-β1-treated and non-treated A549 cells for collagen imaging. Cells were washed three times with PBS and fixed in 4% formaldehyde solution for 15 min. Cells were made permeable by incubation of 0.1% Triton X-100 for 3 min and washed with PBS. Actin filaments and nuclei were stained with 100 nM Rhodamine Phalloidin (Cytoskeleton, Inc., Denver, CO) and 300 nM DAPI (Molecular Probes, Eugene, OR), respectively, as counter-staining for all samples. The fluorescence images were collected using an IX71 Fluorescence Microscope (Olympus, Tokyo, Japan) and were analyzed using NIH ImageJ software.

2.11. FACS analysis

A549 cells (2×10^5 cells) were seeded in a petri dish (35 × 15 mm) and stimulated with 5 ng/mL of TGF-β1 and 5 μg/mL of L-ascorbic acid for 72 h. For control analysis, A549 cells were seeded in a petri dish (35 × 15 mm) without stimulation. 1.0×10^{10} phage particles, Alexa Fluor® 488 conjugated M13-$7GPP_{III}$-HPQ_{VIII} phages and Alexa Fluor® 488 conjugated M13-HPQ_{VIII} (control), were added to A549 cells (5×10^5 cells) in 1 mL of PBS, and the mixture was incubated for 2 h at 37 °C. After incubation, cells were washed three times with PBS. Phage binding was detected by FACScalibur (Becton Dickinson, San Jose, CA). For each sample, 10,000 cells were analyzed with FACScalibur using FlowJo software (Treestar, Inc., San Carlos, CA).

2.12. Statistical analysis

All results from *in vitro* experiments were expressed as mean ± SD of three independent experiments. When it was necessary to compare the means between treatments, an unpaired Student's *t*-test was applied to analyze the data. Comparison among multiple groups was performed using one-way ANOVA with the Tukey test. $p < 0.05$ was considered to be the minimal level of significance.

3. Results

3.1. Construction of the desired CMP engineered M13 phage

We constructed a phage to express both CMP and streptavidin binding peptide using recombinant DNA techniques. For collagen-targeting purpose, the $(GPP)_n$ peptide was engineered on pIII of M13-Wild (M13-$2GPP_{III}$, M13-$4GPP_{III}$, M13-$6GPP_{III}$, and M13-$7GPP_{III}$) (Supplementary Table S1). The phages were engineered with the streptavidin binding peptide on pVIII (M13-HPQ_{VIII}). These streptavidin binding peptides allow for the conjugation of functional motifs such as therapeutic or imaging agents through streptavidin conjugation [40,41]. We confirmed the DNA sequences and locations for both HPQ and $(GPP)_n$ peptides (Supplementary Fig. S1). The resulting phage (M13-$7GPP_{III}$-HPQ_{VIII}) displayed a high density of HPQ peptides (2700 copies/phage) on the major coat proteins and five copies of the nGPP peptides on the pIII minor coat proteins (Fig. 1). We used engineered phages with only HPQ on pVIII (M13-HPQ_{VIII}) or M13-Wild as controls.

3.2. Binding characterization of the CMP engineered phage on collagens

In order to measure the binding affinity of the CMP engineered phage (M13-$nGPP_{III}$), we prepared differently structured collagen thin films and characterized the CMP engineered phage binding on them. Type I collagen self-assembly *in vitro* is an entropy driven process via loss of surface bound solvent molecules [42]. Collagen fibrils self-assemble into different structures depending on pH and electrolyte concentrations in the buffered solutions [43,44]. We prepared two different collagen morphology samples shown in Fig. 2A and B. Collagen thin film samples prepared in pH3.0 buffered condition exhibited highly disrupted fibrillar structures (Fig. 2A). The collagen films prepared pH6.0 buffered condition exhibit normal collagen banded structures with the characteristic 67 nm collagen band structures (Fig. 2B). Therefore, we used these two films for the collagen model targets in the binding assays.

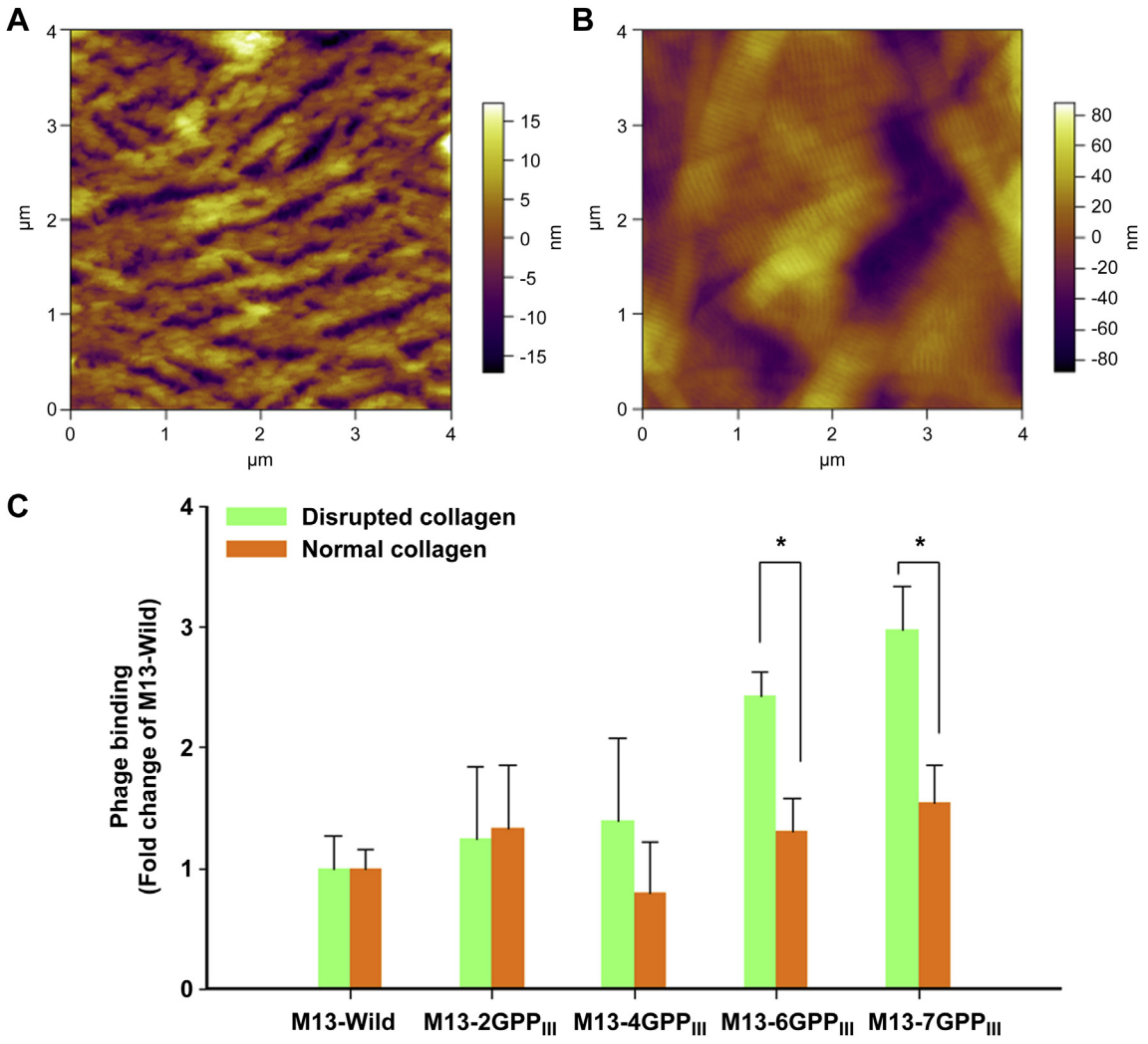

Fig. 2. Characterization of the CMP engineered phage on collagen films. AFM images of collagen thin films prepared at (A) 0.1 M citrate buffer (pH 3) and (B) 0.1 M citrate buffer (pH 6). Collagen bundles are highly disrupted structures at 0.1 M citrate buffer (pH 3) with highly branched structures (A). Normal collagen structure at 0.1 M citrate buffer (pH 6) with characteristic collagen bands exhibiting ~67 nm bands (B). (C) CMP engineered phage, M13-6GPP$_{III}$ and 7GPP$_{III}$, bind on disrupted collagen at a significantly higher levels than on normal collagen (*, $p < 0.01$). Data represent the mean ± SD of three independent experiments.

In order to measure the binding affinity of the CMP engineered phage, we investigated the CMP engineered phage binding on disrupted collagen and normal collagen using ELISA assay. Briefly, 1.0×10^{10} phages/mL of each phage was incubated on those collagen films for 1 h at 37 °C, and the bound phages were measured using HRP-conjugated anti-M13 monoclonal antibody. As the CMP length on the phages was increased, the binding of phages on disrupted collagen was increased. No increase was observed for normal collagen (Fig. 2C). M13-6GPP$_{III}$ and M13-7GPP$_{III}$ showed significantly higher binding on disrupted collagen than on normal collagen ($p < 0.01$) (Fig. 2C).

We investigated the engineered phage binding capability on disrupted collagen using ELISA assay in the concentration range of 2.5×10^{6}–1.0×10^{13} phages/mL. Based on the ELISA assays, we evaluated the binding affinity of phages by calculating the phage concentration at which the binding is 50% of maximum binding (K_d: the equilibrium dissociation constant) with the Hill equation, as seen in Fig. 3. The mean K_d value was 1.5×10^{10} phages/mL for M13-7GPP$_{III}$ and 2.4×10^{11} phages/mL for M13-Wild, suggesting the affinity of M13-7GPP$_{III}$ was about 16 times higher than the affinity of M13-Wild phage on disrupted collagen. As GPP repeats on the minor coat protein (n = 2, 4, 6, and 7) were increased, the binding affinity to the disrupted collagen was also enhanced. The mean dissociation constants for the CMP engineered phage (M13-nGPP$_{III}$) for the disrupted collagen were 3.9×10^{11}, 5.8×10^{10}, 2.9×10^{10}, and 1.5×10^{10} phages/mL for n = 2, 4, 6, and 7, respectively (Fig. 3). There was no significant difference between M13-Wild and M13-2GPP$_{III}$ (K_d, $2.4 \times 10^{11} \pm 2.5 \times 10^{10}$ phages/mL for M13 wild and $3.9 \times 10^{11} \pm 2.0 \times 10^{11}$ phages/mL for M13-2GPP$_{III}$). CMP phage binding to BSA was negligible (Fig. 3). Because the M13-7GPP$_{III}$ exhibited the highest binding affinity for the target collagen, we used the M13-7GPP$_{III}$ for the further characterization.

3.3. Evaluation of the CMP-phage binding on denatured collagens

We characterized collagen binding of M13-7GPP$_{III}$ phages on various collagen structures including normal and denatured collagens (disrupted, heat-denatured, and MMP1-treated collagens). We prepared each collagen films using drop-cast films and characterized their binding with the M13-7GPP$_{III}$ by ELISA assay and compared it to those of M13-Wild (as control). M13-7GPP$_{III}$ phage was bound 2.1-, 5.6-, 9.4-, and 8.0- times more on normal, disrupted, heat-denatured, and MMP1-treated collagens, respectively, than M13-Wild phage (Fig. 4). M13-7GPP$_{III}$ phage can be bound more to

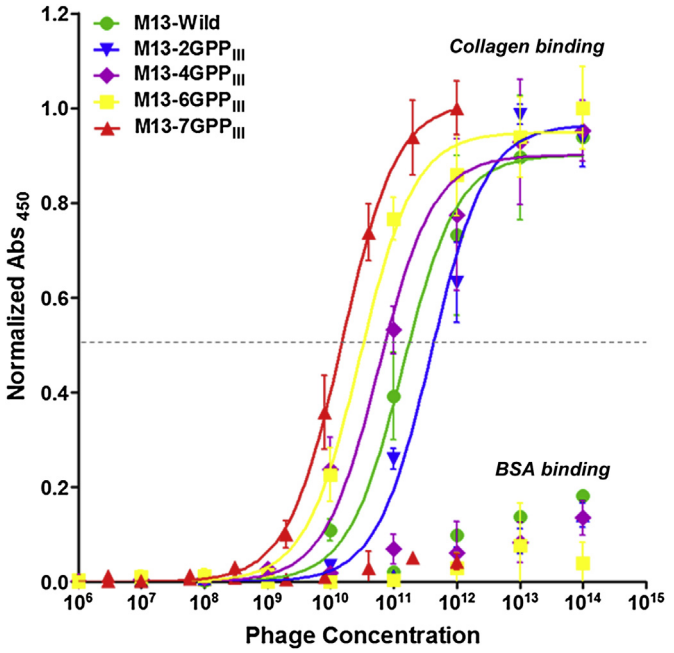

Fig. 3. Binding characterization of the CMP engineered phages. Binding activity of the CMP engineered phages to disrupted rat tail collagen type I or BSA was detected using HRP-conjugated anti-M13 phage antibody. Solid lines represent fits to the Hill equation. Error bars represent the mean ± SD of three independent experiments.

disrupted collagen than normal collagen and can be bound the most to heat-denatured collagen (unstructured collagen, $p < 0.001$) and collagen denatured by MMP1 enzyme treatment ($p < 0.001$) (Fig. 4).

3.4. Evaluation of the CMP engineered phage binding on different collagen types

To further investigate binding characteristics of M13-7GPP$_{III}$ phage, we also characterized their binding affinity to various types of collagens. We treated M13-7GPP$_{III}$ and M13-Wild (i.e., control) phages on rat type I, human type I, bovine type II, and human type III–V, and quantitatively measure the bound phage amount using ELISA assay. Because the GPP repeats can be associated to denatured parts of collagen fibrils, we tested our engineered phage binding on fibrillar collagens (collagen type I, II, III, and V), non-fibrillar collagen (collagen type IV) and laminin (ECM protein) [45]. The M13-7GPP$_{III}$ phage exhibited binding affinity to various collagen types (Fig. 5). The M13-7GPP$_{III}$ showed the best binding on collagen type I and II. The M13-7GPP$_{III}$ phage was bound to fibrillar collagen types, 4.4-, 5.6-, 4.8- times more than M13-Wild phage on rat collagen type I ($p < 0.01$), human type I ($p < 0.05$), and bovine type II ($p < 0.05$), respectively. M13-7GPP$_{III}$ phage was bound to other fibrillar collagen types 2.5- and 2.8-times more than M13-Wild phage on human collagen type III ($p < 0.05$) and V ($p < 0.05$), respectively. M13-7GPP$_{III}$ phage was bound to human collagen type 4, non-fibrillar collagen, 1.9 times more than M13-Wild phage ($p < 0.05$) (Fig. 5). However, M13-7GPP$_{III}$ phage was rarely bound to laminin, an extracellular matrix (ECM) protein, indicating that M13-7GPP$_{III}$ phage could bind to collagens selectively.

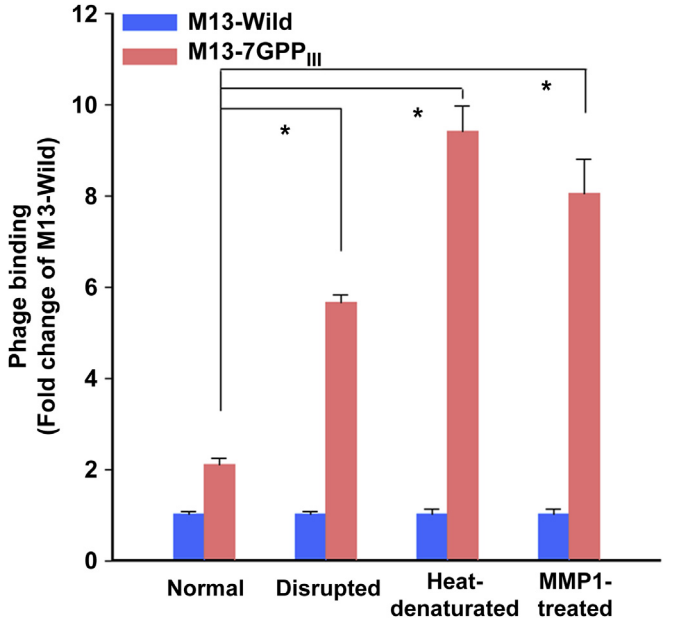

Fig. 4. The CMP phage, M13-7GPP$_{III}$, binding on rat collagen type I with different denatured methods. M13-7GPP$_{III}$ bound significantly more to unstructured collagens (disrupted, MMP1-digested, and heat-denatured) than to normal collagen (*, $p < 0.001$).

3.5. The CMP engineered phage binding on induced abnormal collagen in A549 cells

We investigated the targeting capability of the M13-7GPP$_{III}$ phage using cancer cell lines with controlled collagen expression *in vitro*. We used A549 cells, human lung cancer cells, to control type I collagen expression by TGF-β1. We then performed binding assays in a TGF-β1 dependent manner [39]. In order to induce the collagen expression, the cells were treated with 5 ng/mL of TGF-β1 and 5 μg/mL L-ascorbic acid for 72 h, and the effects on collagen expression were assessed by RT-PCR. The expression of collagen type I was significantly ($p < 0.05$) stimulated as detected by RT-PCR (Fig. 6A) and increased 1.7 times by TGF-β1 as compared to the expression in control cells (Fig. 6B). MMPs expression was examined using gelatin zymography to measure whether the collagen condition of A549 cells had similar characteristics to highly denatured forms for cancer cell migration in response to TGF-β1 treatment [39]. Gelatin zymography was performed using the cell

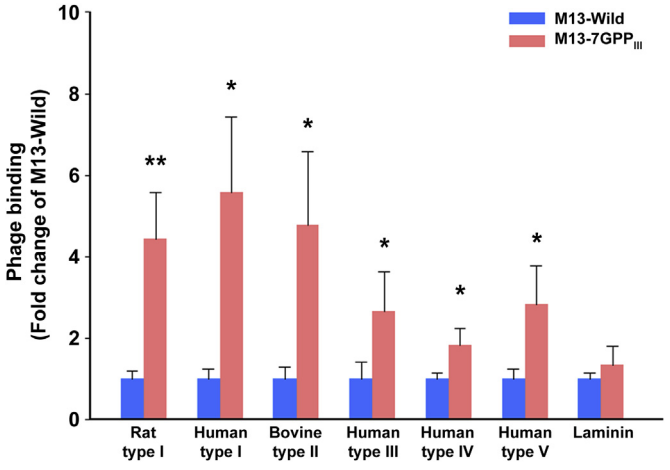

Fig. 5. Binding characteristics of the CMP phage (M13-7GPP$_{III}$) on various collagen types and laminin. M13-7GPP$_{III}$ was able to bind various collagen types effectively. Various collagen types (rat collagen type I, human type I, bovine type II, human type III, IV, and V (10 μg/well)) were coated on a 96-well plate. Phage binding was measured by ELISA assay. Phage binding is expressed as fold-changes compared to the control. Each error bar represents the mean ± SD of three independent experiments. *$p < 0.05$, **$p < 0.01$.

culture media that were harvested after 72 h of TGF-β1 treatment (5 ng/mL). The samples were applied to a 10% polyacrylamide gel containing gelatin without reduction, and proteolytic activity was demonstrated by digestion of the gelatin and clearing of the gel. The A549 cells secreted gelatinases with molecular weights consistent to an identity of MMP-2 and MMP-9 (Fig. 6C). MMP-2 was the major gelatinase expressed, and the TGF-β1 treatment up-regulated MMP-2 expression in the cell culture media. Basal MMP-9 expression was low, and its expression was not changed by TGF-β1 treatment (Fig. 6C).

TGF-β1 was used to induce abnormal collagen in A549 cells, and phage binding (1.0×10^{10} phages/mL) was measured by ELISA assay (Fig. 6D). M13-7GPP$_{III}$ phage was bound to collagen 1.5 times more than M13-Wild phage on the surface of A549 cells without collagen induction by TGF-β1. In cancerous, collagen over-expressed A549 cells, M13-7GPP$_{III}$ phage bound up to 3.7 times more than the control phage, while the collagen expression was increased 1.7 times (Fig. 6B and D). This enhanced binding of 7GPP$_{III}$ phage suggested that the M13-7GPP$_{III}$ phage could bind more effectively to abnormal collagens than to normal collagen (Fig. 6D).

3.6. Fluorescence imaging and FACS analysis for abnormal collagen by the CMP engineered phage

After confirmation of the effective binding of the M13-7GPP$_{III}$ on the A549 cells in a TGF-β1 dependent manner, we imaged the A549 cells using the phage engineered with both CMP and streptavidin binding HPQ peptides. Streptavidin-Alexa Fluor®488 was bound to the HPQ peptides of M13-7GPP$_{III}$-HPQ$_{VIII}$ by the simple mixing of streptavidin-Alexa Fluor®488 (5 mol dye/mole) and HPQ-displayed phages solutions. Loading amounts of streptavidin-Alexa Fluor®488 per phage were quantified by the absorbance of the phage–Alexa Fluor®488 conjugate at 269 and 495 nm. Each phage carried an average of 275 Alexa Fluor®488 molecules. Because five dyes are conjugated with a streptavidin, the UV–Vis result indicate that ~2% of the HPQ peptides on the pVIII major coat protein were functionalized with streptavidin-Alexa Fluor®488 among the 2700 copies of the HPQ peptide on major coat protein.

To evaluate the engineered phage as an imaging agent, we treated Alexa Fluor®488-tagged M13-7GPP$_{III}$-HPQ$_{VIII}$ phage or Alexa Fluor®488-tagged M13-HPQ$_{VIII}$ (control) on A549 cells with or without collagen induction. The same amount of each fluorescent phage (1.0×10^{10} phages/mL) was treated in the three different wells of A549 cells for 1 h at 37 °C. Representative images are shown in Fig. 7. Control phages (M13-HPQ$_{VIII}$) without collagen binding motif (7GPP) were not significantly bound to collagens on the surface of A549 cells both with and without TGF-β1 treatment (Image A3 and C3 in Fig. 7). We observed that the A549 cells without TGF-β1 treatment incubated with Alexa Fluor®488-tagged M13-7GPP$_{III}$-HPQ$_{VIII}$ phage still exhibited phage binding because A549 cells without TGF-β1 treatment also expressed some collagens (Figs. 6D and Fig. 7-B3). However, the Alexa Fluor®488-tagged M13-7GPP$_{III}$-HPQ$_{VIII}$ provided the best images of the abnormal collagens on TGF-β1 treated A549 cells; it was consistent with cell shapes as compared to the actin image (Fig. 7-D3).

Using Alexa Fluor®488-tagged M13-HPQ$_{VIII}$ phage (control) and M13-7GPP$_{III}$-HPQ$_{VIII}$ phage, abnormal collagen induced A549 cells were detected by FACS. Alexa Fluor®488-tagged M13-HPQ$_{VIII}$ phage or M13-7GPP$_{III}$-HPQ$_{VIII}$ phage were incubated in control A549 cells without collagen induction. The fluorescence histogram of M13-7GPP$_{III}$-HPQ$_{VIII}$ phage incubated A549 cells was slightly increased while the histogram of M13-HPQ$_{VIII}$ phage incubated A549 cells

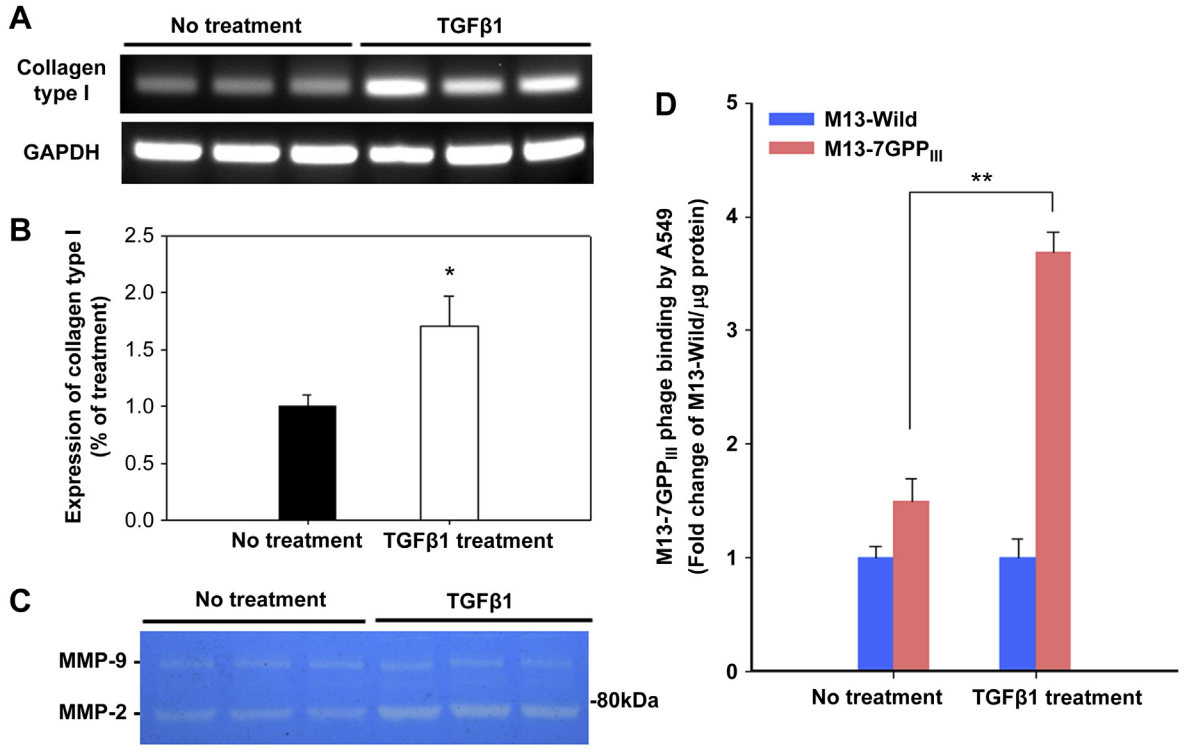

Fig. 6. Binding characteristics of the CMP phage (M13-7GPP$_{III}$) on collagen expressing A549 cells, induced by TGF-β1. A549 cells were incubated with 5 ng/mL TGF-β1 in the presence of 5 μg/ml L-ascorbic acid for 72 h (A) mRNA expression of collagen type I was detected by RT-PCR. (B) Densitometric analysis of Fig. 6A was performed by ImageJ. The changes in expression level are expressed as fold-changes compared to the control. Each bar represents the mean ± SD of three independent experiments. $^{*}p < 0.05$. (C) Measurement of MMP-2 and MMP-9 activities in cell culture media after 72 h of TGF-β1 treatment by enzyme zymography. MMP-2 activity was significantly increased by TGF-β1, and MMP-9 activity was unchanged. (D) M13-7GPP$_{III}$ phage was bound more to TGF-β1-induced collagen in A549 cells than in control cells. Each error bar represents the mean ± SD of three independent experiments. $^{**}p < 0.001$.

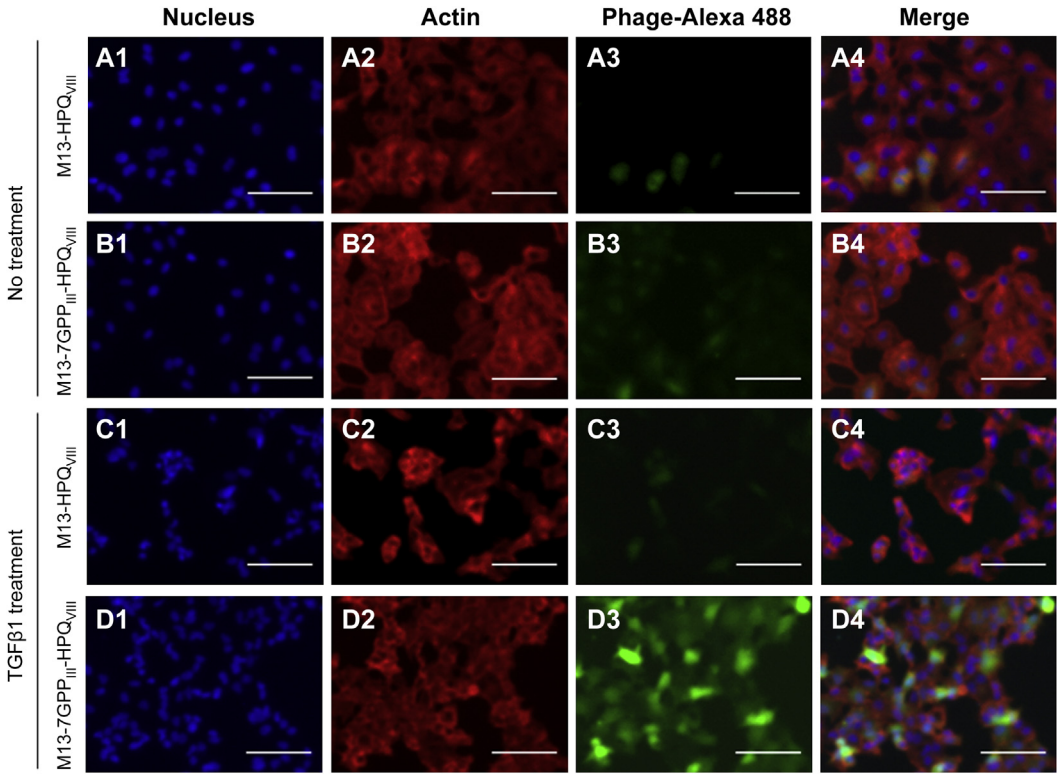

Fig. 7. The fluorescent labeled engineered phage (M13 -7GPP$_{III}$-HPQ$_{VIII}$) can image collagen in human lung cancer cells, A549. Abnormal collagen in A549 cells were induced by treatment with 5 ng/mL TGF-β1 in the presence of 5 μg/mL L-ascorbic acid for 72 h (C and D). The control group received no treatment (A and B). Cells were incubated with either Alexa Fluor®488 conjugated M13-HPQ$_{VIII}$ (as a control) (A and C) or Alexa Fluor®488 conjugated M13-7GPP$_{III}$-HPQ$_{VIII}$ phage (B and D). (1) Blue: DAPI, nucleus; (2) Red: actin filaments; (3) Green: phages-Alexa Fluor®488; (4) composite images of 1, 2, and 3. Scale bar = 100 μm. (For interpretation of the references to color in this figure legend, the reader is referred to the web version of this article.)

was similar to that of A549 cells without phage incubation in FACS histogram (Fig. 8A). Mean fluorescence intensity (MFI) values in control A549 cells without TGF-β1 treatment were 18.1 ± 3.6, 12.8 ± 4.0, and 25.1 ± 4.5 for control A549 only, M13-HPQ$_{VIII}$, and M13-7GPP$_{III}$-HPQ$_{VIII}$, respectively (Fig. 8A). Percentages of abnormal collagen positive cells were 1.4 ± 0.4% for M13-HPQ$_{VIII}$ and 2.1 ± 0.8% for M13-7GPP$_{III}$-HPQ$_{VIII}$ compared to the control cells (Fig. 8A). Alexa Fluor®488-tagged M13-HPQ$_{VIII}$ phage or M13-7GPP$_{III}$-HPQ$_{VIII}$ phage was incubated in abnormal collagen induced A549 cells by TGF-β1 treatment. Only the fluorescence histogram of M13-7GPP$_{III}$-HPQ$_{VIII}$ phage incubated A549 cells was increased and shifted to right-side in FACS histogram (Fig. 8B). MFI values in

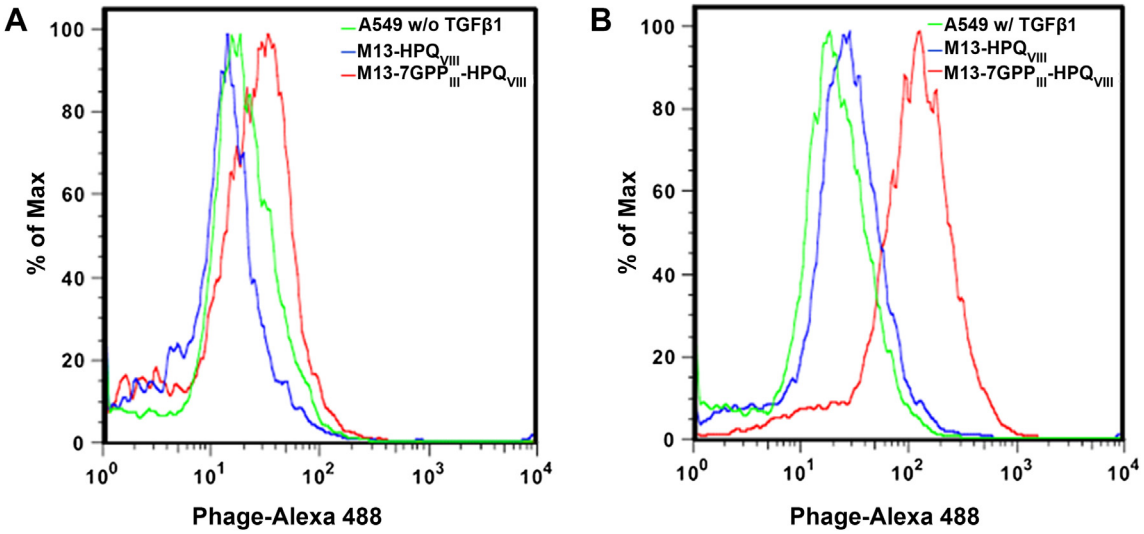

Fig. 8. FACS histogram of induced abnormal collagen detection by Alexa Fluor®488-tagged M13-7GPP$_{III}$-HPQ$_{VIII}$ in A549 cells without treatment (A) and with TGF-β1 treatment (B). Green: A549 cells without phage, Blue: Alexa Fluor®488 conjugated M13-HPQ$_{VIII}$ (control), Red: Alexa Fluor®488-tagged M13-7GPP$_{III}$-HPQ$_{VIII}$ phage incubation. (For interpretation of the references to color in this figure legend, the reader is referred to the web version of this article.)

collagen induced A549 cells by TGF-β1 treatment were 19.8 ± 4.1, 26.7 ± 5.4, and 121 ± 22.4 for collagen induced A549 cells only, M13-HPQ_{VIII}, and M13-$7GPP_{III}$-HPQ_{VIII}, respectively (Fig. 8B). Percentages of abnormal collagen positive cells were 4.8 ± 1.2% for M13-HPQ_{VIII} and 60.5 ± 8.8% for M13-$7GPP_{III}$-HPQ_{VIII} compared to the control cells (Fig. 8B). There was no significant difference between M13-HPQ_{VIII} phage incubated A549 cells and A549 cells only (Fig. 8B).

4. Discussion

M13 phage possesses multiple advantageous structural features for biomedical materials. The phage is nonpathogenic to human cells and easily removed from the body with little side-effect [46–48]. Large quantities of identical phage coat proteins can be easily produced by amplification in bacterial host cells and self-assembled to form a nanofibrous shape. In addition, its minor (pIII, pVI, pVIII and pIX) and major (pVIII) coat proteins can be modified to display functional peptide motives by genetic or chemical modification [32–35]. In this paper, we developed genetically engineered M13 phage (M13-$7GPP_{III}$-HPQ_{VIII}) that could be used as an imaging agent to target collagen in cancer cells. We showed that by expressing collagen mimetic peptide on the minor coat protein (M13-$7GPP_{III}$) collagen binding of M13-$7GPP_{III}$ was dramatically enhanced compared with that of M13-Wild phage (Figs. 2C and 3). Moreover, the addition of streptavidin binding peptide (HPQ) on pVIII did not interrupt the function of 7GPP and provided 2700 copies of motives to bind a streptavidin-conjugated imaging agent. We were able to successfully image and detect the cancer collagen using M13-$7GPP_{III}$-HPQ_{VIII} (Figs. 7 and 8). In the future, we can use our engineered M13 phage as a drug delivery vehicle through conjugation with therapeutic drugs.

The hierarchical organization of collagen molecules provides superior mechanical properties to connective tissues (e.g., ligaments, tendons, etc.) [49], forms extracellular matrices (e.g., cartilage, cornea, etc.) [50], and is important for several biological functions such as tissue-structuring, cell attachment, tissue repair, and control of tissue-related diseases [51,52]. Collagen mimetic peptides (CMPs) are typically less than 30 amino acids and contain the repeat tripeptide sequences Gly-Pro-Pro and/or Gly-Hyp-Pro. The CMP is known to bind or hybridize with denatured collagen by associating with disentangled parts of the collagen molecules [3,36,37]. Therefore, we hypothesized that CMPs on the M13-$7GPP_{III}$ phage would bind more to highly denatured collagen structures present in diseases like cancers than to normal collagens (Fig. 1).

We constructed two different structures of collagen fibrils to reflect normal collagen and disrupted collagen by controlling the pH condition of the buffer solutions used to characterize the CMP engineered phages (Fig. 2A, B) [25,43,53–55]. M13-$7GPP_{III}$ phage exhibited higher binding on the disrupted collagen film prepared in pH3 than on the normal collagen film in pH6 ($p < 0.01$) (Fig. 2C). It exhibited a 16 times increased binding affinity on disrupted collagen compared to M13-Wild phage (Fig. 3). This indicates that CMP motives displayed on the M13 phage can be successfully functionalized and can bind to disrupted collagen more than to normal collagen. Furthermore, in order to emulate more disease conditions with disrupted collagen molecular structure, heat-denatured (gelatin) and MMP digested collagen were added to normal and disrupted rat collagen type I. Heat-denatured collagen is characterized by randomly denatured collagen molecules and an unstructured form through the structural degradation of collagen [56]. MMP can change the molecular structure of collagen in human disease by cleaving all three polypeptide chains of the 300 nm triple-helical collagen monomer at a specific recognition site ~225 nm from the N-terminus of collagen molecules. The resulting collagen molecules cleaved into two collagen fragments have melting temperatures around 34 °C and can be further denatured and structurally changed at body temperature [53,57,58]. Therefore, we evaluated M13-$7GPP_{III}$ phage binding ability to normal and disrupted forms of rat collagen type I, as well as collagen denatured by heat or by MMP enzyme digestion. We observed that the level of M13-$7GPP_{III}$ binding was as low as the level of M13-Wild binding on normal collagen and that M13-$7GPP_{III}$ exhibited approximately 5.6–9.4- times higher levels of binding after 37 °C incubation on disrupted, MMP-1 treated, and heat-denatured (gelatin) collagens compared to M13-Wild (Fig. 4). This binding result suggested that M13-$7GPP_{III}$ phage preferred to bind to denatured collagens than to normal collagen and might be used for collagen targeting in disease conditions.

We investigated the collagen binding affinity of CMP displayed phages (M13-$2GPP_{III}$, $4GPP_{III}$, $6GPP_{III}$, $7GPP_{III}$ phages) on disrupted collagen. The phages which displayed more GPP repeats showed an increased collagen binding affinity, and the engineered phages needed more than 4GPP repeats on their minor coat in order to bind significantly more to disrupted collagen than to normal collagen (Figs. 2C and 3). We compared the dissociation constants (K_d) of the CMP phages with the Hill equation. As the GPP repeat number increased, the binding affinity (K_d) of M13-nGPP phage was enhanced (Fig. 3). The M13-$7GPP_{III}$ phage has the best binding affinity (16 times stronger than M13-Wild) on disrupted collagen than the other CMP phages (Fig. 4). In order to obtain an even higher binding affinity for collagen, we tried to construct longer CMP-displayed M13 phages, such as 8GPP or 10GPP. However, 7GPP was the longest CMP-displayed M13 phage we could construct so far. We assume that gene deletion might be occurring while the phage is replicated in *Escherichia coli* cells because the repeated Gly-Pro-Pro amino acid sequences are made of a high number of guanine (G) and cytosine (C) repeats in their respective codons (i.e., GGN-CCN-CCN for GPP amino acids). Highly repeated guanine (G) and cytosine (C) sequences might make hairpin structures which can be easily deleted during DNA duplication in *E. coli* cells undergoing phage cloning [59]. For example, when we were constructing M13-$7GPP_{III}$ phages, shorter GPP phages were also constructed because of gene deletion (data not shown). Although 7GPP is the longest CMP that could be displayed on the minor coat of M13 phage, the Yu group has reported that the binding affinity of CMP-7 and CMP-10 are similar (1.7×10^{-8} M for CMP-7 and 1.4×10^{-8} M for CMP-10, respectively) for disrupted collagen film [60]. Therefore, we expect that the binding affinity of the M13 phage with CMP-7 and CMP-10 might be similar [60]. The Meijer group showed that dendrimers functionalized with collagen binding peptides in a pentavalent manner could bind 100 times stronger than that of a monomeric dendrimer [61]. M13 phage also displays five copies of CMP on their minor coat protein. Therefore, we expect that M13-$7GPP_{III}$ phage could multivalently bind to collagen and exhibit enhanced binding affinity like pentameric dendrimer.

To conjugate imaging agents on the engineered phage, streptavidin binding peptide (HPQ) was displayed on the pVIII major coat protein of M13-$7GPP_{III}$ phage. The HPQ-peptide, which specifically binds to streptavidin, was previously identified using phage display [40,41,62]. We engineered the phage to display a linear peptide, FSHPQNT (K_d = 125 μM for streptavidin) [40,41]. It displayed 2700 copies of HPQ peptide, densely and uniformly, on its major coat (HPQ_{VIII}). We prepared Alexa Flour®488 tagged phages after simple mixing of M13-$7GPP_{III}$-HPQ_{VIII} phage and streptavidin-Alexa Flour®488. We could conjugate ~2% of the HPQ peptides on the CMP phage with streptavidin-Alexa Flour®488 for imaging. This simple imaging probe modification is an advantageous way to

prepare various imaging agents and could be extended to therapeutic molecule conjugation.

Human lung cancer cells, A549 cells, were treated with TGF-β1 and L-ascorbic acid to induce collagen expression [39]. Not only collagen type I was increased in cells, but matrix metalloproteinase-2 (MMP-2) was also increased in the cell culture media, suggesting that collagens on the surface of A549 cells were highly digested and denatured by MMP-2 after the 72-hr TGF-β1 treatment (Fig. 6A–C) [17,39]. M13-7GPP$_{III}$-HPQ$_{VIII}$ phage attached to A549 cells with denatured collagens 3.7 times more than to A549 cells without treatment (Fig. 6D). This result indicates that M13-7GPP$_{III}$-HPQ$_{VIII}$ phage could attach more to cancer cells and tissues with collagen remodeling than to normal cells. Alexa Flour®488 tagged M13-7GPP$_{III}$-HPQ$_{VIII}$ phages were successfully bound to abnormal collagen in A549 cells (Fig. 7-D3). Fluorescence signals of phages were similar to those of actin filaments because collagen covered the entire surface of the A549 cells (Fig. 7-B2 and B3, D2 and D3). This suggests that our M13-7GPP$_{III}$-HPQ$_{VIII}$ phages could be useful for cancer collagen imaging. Moreover, we detected the abnormal collagen in A549 cells using Alexa Flour®488 tagged M13-7GPP$_{III}$-HPQ$_{VIII}$ phages by FACS (Fig. 8). When Alexa Fluor®488-tagged engineered phages were incubated in abnormal collagen induced A549 cells by TGF-β1 treatment, the fluorescence histogram of M13-7GPP$_{III}$-HPQ$_{VIII}$ phage incubated A549 cells was increased and shifted to right-side in FACS histogram (Fig. 8B). There was no significant difference between M13-HPQ$_{VIII}$ phage incubated A549 cells and A549 cells only (Fig. 8A and B). Therefore, the M13-7GPP$_{III}$-HPQ$_{VIII}$ phage could selectively distinguish the abnormal collagen over-expressed cancer cells through fluorescent labeling. In previous research for molecular imaging of cancer using engineered phages, several peptides were successfully used to image cancer such as $\alpha_v\beta_3$-integrin-binding RGD containing peptides [21], VHSPNKK peptide for VCAM-1 (vascular cell adhesion molecule 1) expressing tumor endothelial cells [63], SPPTGIN peptide for SPARC up-regulated in invasive cancer [64]. In addition, our 7GPP peptide-displayed phage for abnormal collagen might be a potential biomaterial for targeting and for use as imaging agents in various cancers.

5. Conclusions

In summary, we developed collagen-mimetic peptide (CMP) engineered phage for collagen targeting and imaging in cancers. We genetically engineered M13 phage to stably express both the CMP motif $(Gly\text{-}Pro\text{-}Pro)_7$ on the minor coat proteins and the streptavidin-binding peptide (HPQ) on the major coat proteins. This construct, M13-7GPP$_{III}$-HPQ$_{VIII}$, was able to selectively bind several types of collagen using five copies of the CMP motif. The collagen binding efficiency of M13-7GPP$_{III}$-HPQ$_{VIII}$ phage on disrupted collagen was improved by 16 times compared to that of the M13-Wild phage. Moreover, M13-7GPP$_{III}$-HPQ$_{VIII}$ phage can bind more to TGF-β1-induced abnormal collagen in A549 cells than in control cells. HPQ-peptide on the major coat protein of M13-7GPP$_{III}$-HPQ$_{VIII}$ can be easily attached to fluorescent imaging agents through streptavidin conjugation. We believe that our CMP engineered phage could be used as a collagen targeting agent to detect and image the numerous pathological conditions related to abnormal collagen remodeling in the future.

Acknowledgments

H.E.J. was supported by Basic Science Research Program through the National Research Foundation of Korea (NRF) funded by the Ministry of Education, Science and Technology (NRF-2011-357-E00083).

Appendix A. Supplementary data

Supplementary data related to this article can be found online at http://dx.doi.org/10.1016/j.biomaterials.2014.07.044.

References

[1] Even-Ram S, Yamada KM. Cell migration in 3D matrix. Curr Opin Cell Biol 2005;17:524–32.
[2] Gelse K, Poschl E, Aigner T. Collagens – structure, function, and biosynthesis. Adv Drug Deliv Rev 2003;55:1531–46.
[3] Li Y, Foss CA, Summerfield DD, Doyle JJ, Torok CM, Dietz HC, et al. Targeting collagen strands by photo-triggered triple-helix hybridization. Proc Natl Acad Sci U S A 2012;109:14767–72.
[4] Won S, Davies-Venn C, Liu S, Bluemke DA. Noninvasive imaging of myocardial extracellular matrix for assessment of fibrosis. Curr Opin Cardiol 2013;28:282–9.
[5] Provenzano PP, Eliceiri KW, Campbell JM, Inman DR, White JG, Keely PJ. Collagen reorganization at the tumor-stromal interface facilitates local invasion. BMC Med 2006;4:38.
[6] Conklin MW, Eickhoff JC, Riching KM, Pehlke CA, Eliceiri KW, Provenzano PP, et al. Aligned collagen is a prognostic signature for survival in human breast carcinoma. Am J Pathol 2011;178:1221–32.
[7] Saftlas AF, Hoover RN, Brinton LA, Szklo M, Olson DR, Salane M, et al. Mammographic densities and risk of breast cancer. Cancer 1991;67:2833–8.
[8] Saftlas A, Hoover R, Brinton L, Szklo M, Wolfe J. Mammographic densities as indicators of breast-cancer risk. Am J Epidemiol 1988;128:914.
[9] Liang Y, Diehn M, Bollen AW, Israel MA, Gupta N. Type I collagen is overexpressed in medulloblastoma as a component of tumor microenvironment. J Neurooncol 2008;86:133–41.
[10] Santala M, Simojoki M, Risteli J, Risteli L, Kauppila A. Type I and type III collagen metabolites as predictors of clinical outcome in epithelial ovarian cancer. Clin Cancer Res 1999;5:4091–6.
[11] Ohlund D, Lundin C, Ardnor B, Oman M, Naredi P, Sund M. Type IV collagen is a tumour stroma-derived biomarker for pancreas cancer. Br J Cancer 2009;101:91–7.
[12] Skovbjerg H, Anthonsen D, Lothe IMB, Tveit KM, Kure EH, Vogel LK. Collagen mRNA levels changes during colorectal cancer carcinogenesis. BMC Cancer 2009;9.
[13] Ramshaw JAM, Shah NK, Brodsky B. Gly-X-Y tripeptide frequencies in collagen: a context for host-guest triple-helical peptides. J Struct Biol 1998;122:86–91.
[14] Brodsky B, Persikov AV. Molecular structure of the collagen triple helix. Adv Protein Chem 2005;70:301–39.
[15] Nagase H, Visse R. In: Parks WC, Mecham RP, editors. Triple helicase activity and the structural basis of collagenolysis. Extracellular matrix degradation, biology of extracellular matrix. Heidelberg: Springer; 2011. p. 95–122.
[16] Brinckerhoff CE, Matrisian LM. Timeline – matrix metalloproteinases: a tail of a frog that became a prince. Nat Rev Mol Cell Biol 2002;3:207–14.
[17] Page-McCaw A, Ewald AJ, Werb Z. Matrix metalloproteinases and the regulation of tissue remodelling. Nat Rev Mol Cell Biol 2007;8:221–33.
[18] Egeblad M, Werb Z. New functions for the matrix metalloproteinases in cancer progression. Nat Rev Cancer 2002;2:161–74.
[19] Brinckerhoff CE, Rutter JL, Benbow U. Interstitial collagenases as markers of tumor progression. Clin Cancer Res 2000;6:4823–30.
[20] Provenzano PP, Inman DR, Eliceiri KW, Knittel JG, Yan L, Rueden CT, et al. Collagen density promotes mammary tumor initiation and progression. BMC Med 2008;6:11.
[21] Hajitou A, Trepel M, Lilley CE, Soghomonyan S, Alauddin MM, Marini FC, et al. A hybrid vector for ligand-directed tumor targeting and molecular imaging. Cell 2006;125:385–98.
[22] Bhattarai SR, Yoo SY, Lee SW, Dean D. Engineered phage-based therapeutic materials inhibit *Chlamydia trachomatis* intracellular infection. Biomaterials 2012;33:5166–74.
[23] Yoo SY, Merzlyak A, Lee SW. Facile growth factor immobilization platform based on engineered phage matrices. Soft Matter 2011;7:1660–6.
[24] Farr R, Choi DS, Lee SW. Phage-based nanomaterials for biomedical applications. Acta Biomater 2013;10:1741–50.
[25] Chung WJ, Oh JW, Kwak K, Lee BY, Meyer J, Wang E, et al. Biomimetic self-templating supramolecular structures. Nature 2011;478:364–8.
[26] Merzlyak A, Indrakanti S, Lee SW. Genetically engineered nanofiber-like viruses for tissue regenerating materials. Nano Lett 2009;9:846–52.
[27] Choi DS, Jin HE, Yoo SY, Lee SW. Cyclic RGD peptide incorporation on phage major coat proteins for improved internalization by HeLa cells. Bioconjug Chem 2014;25:216–23.
[28] Smith GP, Petrenko VA. Phage display. Chem Rev 1997;97:391–410.
[29] Merzlyak A, Lee SW. Engineering phage materials with desired peptide display: rational design sustained through natural selection. Bioconjug Chem 2009;20:2300–10.
[30] Yoo SY, Kobayashi M, Lee PP, Lee SW. Early osteogenic differentiation of mouse preosteoblasts induced by collagen-derived DGEA-peptide on nanofibrous phage tissue matrices. Biomacromolecules 2011;12:987–96.

[31] Ghosh D, Lee Y, Thomas S, Kohli AG, Yun DS, Belcher AM, et al. M13-templated magnetic nanoparticles for targeted in vivo imaging of prostate cancer. Nat Nanotechnol 2012;7:677–82.
[32] Yoo SY, Chung WJ, Kim TH, Le M, Lee SW. Facile patterning of genetically engineered M13 bacteriophage for directional growth of human fibroblast cells. Soft Matter 2011;7:363–8.
[33] Ghosh D, Kohli AG, Moser F, Endy D, Belcher AM. Refactored M13 bacteriophage as a platform for tumor cell imaging and drug delivery. ACS Synth Biol 2012;1:576–82.
[34] Frenkel D, Solomon B. Filamentous phage as vector-mediated antibody delivery to the brain. Proc Natl Acad Sci U S A 2002;99:5675–9.
[35] Yoo SY, Oh JW, Lee SW. Phage-chips for novel optically readable tissue engineering assays. Langmuir 2012;28:2166–72.
[36] Wang AY, Mo X, Chen CS, Yu SM. Facile modification of collagen directed by collagen mimetic peptides. J Am Chem Soc 2005;127:4130–1.
[37] Mo X, An YJ, Yun CS, Yu SM. Nanoparticle-assisted visualization of binding interactions between collagen mimetic peptide and collagen fibers. Angew Chem Int Ed 2006;45:2267–70.
[38] Qi D, Scholthof KB. A one-step PCR-based method for rapid and efficient site-directed fragment deletion, insertion, and substitution mutagenesis. J Virol Methods 2008;149:85–90.
[39] Kasai H, Allen JT, Mason RM, Kamimura T, Zhang Z. TGF-beta 1 induces human alveolar epithelial to mesenchymal cell transition (EMT). Respir Res 2005;6:56.
[40] Devlin JJ, Panganiban LC, Devlin PE. Random peptide libraries: a source of specific protein binding molecules. Science 1990;249:404–6.
[41] Weber PC, Pantoliano MW, Thompson LD. Crystal-structure and ligand-binding studies of a screened peptide complexed with streptavidin. Biochemistry-Us 1992;31:9350–4.
[42] Kadler KE, Hojima Y, Prockop DJ. Assembly of collagen fibrils de novo by cleavage of the type I pC-collagen with procollagen C-proteinase. Assay of critical concentration demonstrates that collagen self-assembly is a classical example of an entropy-driven process. J Biol Chem 1987;262:15696–701.
[43] Jiang FZ, Horber H, Howard J, Muller DJ. Assembly of collagen into microribbons: effects of pH and electrolytes. J Struct Biol 2004;148:268–78.
[44] Suzuki Y, Someki I, Adachi E, Irie S, Hattori S. Interaction of collagen molecules from the aspect of fibril formation: acid-soluble, alkali-treated, and MMP1-digested fragments of type I collagen. J Biochem 1999;126:54–67.
[45] Bornstein P, Sage H. Structurally distinct collagen types. Annu Rev Biochem 1980;49:957–1003.
[46] Projan S. Phage-inspired antibiotics? Nat Biotechnol 2004;22:167–8.
[47] Merril CR, Biswas B, Carlton R, Jensen NC, Creed GJ, Zullo S, et al. Long-circulating bacteriophage as antibacterial agents. Proc Natl Acad Sci U S A 1996;93:3188–92.
[48] Zou J, Dickerson MT, Owen NK, Landon LA, Deutscher SL. Biodistribution of filamentous phage peptide libraries in mice. Mol Biol Rep 2004;31:121–9.
[49] Gautieri A, Vesentini S, Redaelli A, Buehler MJ. Hierarchical structure and nanomechanics of collagen microfibrils from the atomistic scale up. Nano Lett 2011;11:757–66.
[50] Holmes DF, Gilpin CJ, Baldock C, Ziese U, Koster AJ, Kadler KE. Corneal collagen fibril structure in three dimensions: structural insights into fibril assembly, mechanical properties, and tissue organization. Proc Natl Acad Sci U S A 2001;98:7307–12.
[51] Myllyharju J, Kivirikko KI. Collagens and collagen-related diseases. Ann Med 2001;33:7–21.
[52] Grinnell F. Fibroblast biology in three-dimensional collagen matrices. Trends Cell Biol 2003;13:264–9.
[53] Orgel JPRO, Irving TC, Miller A, Wess TJ. Microfibrillar structure of type I collagen in situ. Proc Natl Acad Sci U S A 2006;103:9001–5.
[54] Loo RW, Goh MC. Potassium ion mediated collagen microfibril assembly on mica. Langmuir 2008;24:13276–8.
[55] Fang M, Goldstein EL, Matich EK, Orr BG, Holl MMB. Type I collagen self-assembly: the roles of substrate and concentration. Langmuir 2013;29:2330–8.
[56] Kozlov PV, Burdygina GI. The structure and properties of solid gelatin and the principles of their modification. Polymer 1983;24:651–66.
[57] Sarkar SK, Marmer B, Goldberg G, Neuman KC. Single-molecule tracking of collagenase on native type I collagen fibrils reveals degradation mechanism. Curr Biol 2012;22:1047–56.
[58] Fligiel SE, Varani J, Datta SC, Kang S, Fisher GJ, Voorhees JJ. Collagen degradation in aged/photodamaged skin in vivo and after exposure to matrix metalloproteinase-1 in vitro. J Invest Dermatol 2003;120:842–8.
[59] Singh VK, Govindarajan R, Naik S, Kumar A. The effect of hairpin structure on PCR amplification efficiency. Mol Biol Today 2000;1:67–9.
[60] Wang AY, Foss CA, Leong S, Mo X, Pomper MG, Yu SM. Spatio-temporal modification of collagen scaffolds mediated by triple helical propensity. Biomacromolecules 2008;9:1755–63.
[61] Helms BA, Reulen SWA, Nijhuis S, de Graaf-Heuvelmans PTHM, Merkx M, Meijer EW. High-affinity peptide-based collagen targeting using synthetic phage mimics: from phage display to dendrimer display. J Am Chem Soc 2009;131:11683–5.
[62] Katz BA, Cass RT. In crystals of complexes of streptavidin with peptide ligands containing the HPQ sequence the pK(a) of the peptide histidine is less than 3.0. J Biol Chem 1997;272:13220–8.
[63] Kelly KA, Clemons PA, Yu AM, Weissleder R. High-throughput identification of phage-derived imaging agents. Mol Imaging 2006;5:24–30.
[64] Kelly KA, Waterman P, Weissleder R. In vivo imaging of molecularly targeted phage. Neoplasia 2006;8:1011–8.